Temperature and momentum dependence of single-particle properties in hot asymmetric nuclear matter

Ch. C. Moustakidis

Department of Theoretical Physics, Aristotle University of Thessaloniki, 54124 Thessaloniki, Greece

We have studied the effects of momentum-dependent interactions on the single-particle properties of hot asymmetric nuclear matter. In particular, the single-particle potential of protons and neutrons as well as the symmetry potential have been studied within a self-consistent model using a momentum-dependent effective interaction. In addition, the isospin splitting of the effective mass has been derived from the above model. In each case temperature effects have been included and analyzed. The role of the specific parametrization of the effective interaction used in the present work has been investigated. It has been concluded that the behavior of the symmetry potential depends strongly on the parametrization of the interaction part of the energy density and the momentum dependence of the regulator function. The effects of the parametrization have been found to be less pronounced on the isospin mass splitting.

PACS number(s): 21.65.−f, 21.30.Fe, 24.10.Pa, 26.60.−c

I. INTRODUCTION

One of the most interesting problems in nuclear physics is the isovector dependence on nuclear force, which can be found in nuclear symmetry energy, the isovector optical potential, and neutron-proton effective mass splitting. The isovector feature of nuclear forces is crucial to gain a good understanding of neutron stars and exotic nuclear collisions produced at radioactive beam facilities and to describe the structure of exotic nuclei. This interest in the isospin dependence of nuclear forces is of recent date because data for neutron-rich nuclei were rather scarce in the past. The forthcoming new generation of radioactive beam facilities, such as the future GSI Facility for Antiproton and Ion Research (GSI-FAIR), the Rare Isotope Accelerator planned in the USA, and the SPIRAL2 at the Grand Accelerateur National D'Ions Lourds (GANIL), will produce huge amounts of new data for neutron-rich nuclei. Up to now, the isovector dependence of nuclear force has been investigated in heavy-ion collision experiments. The advantage of such kinds of reactions is that they allow testing of nuclear forces at supranormal densities because in intermediate energy compressions of two to three times nuclear saturation density is reached. Nevertheless, the asymmetry of the colliding systems is moderate and therefore the isospin effects on the corresponding observables are moderate as well.

From a theoretical point of view, the predictions for the isospin dependence of nuclear interaction are very different. In general, both microscopic and effective interactions have been extensively used to gain knowledge about the nuclear matter properties in conditions far from equilibrium (hot nuclear matter, high-density behavior, etc.). It is appropriate, therefore, in every case to incorporate temperature and momentum dependence to have a richer interaction and as a consequence be able to produce a more thorough description of nuclear matter properties. Specifically, the determination of the nuclear symmetry energy (NSE) based on microscopic and/or phenomenological approaches is of great interest to nuclear physics and nuclear astrophysics. For instance, it is important for the study of the structure and reactions of neutron-rich nuclei, the Type II supernova explosions, neutron-star mergers, and the stability of neutron stars. So far, the main part of the calculations concerning the density dependence of the SE is related to cold nuclear matter ($T = 0$). However, recently there has been an increasing interest in the study of the properties of asymmetric nuclear matter, including NSE, and the properties of neutron stars at finite temperature [1–21].

In our previous work [21] we studied the effects of finite temperature on NSE and we also found the appropriate relations describing that effect. We especially focused on the interaction part of the NSE, which so far has received little theoretical attention concerning its dependence on temperature. We applied a momentum-dependent effective interaction model. This model, called BGBD (Bombaci-Gale-Bertsch-Das Gupta), was introduced by Gale *et al*. [22–25] to examine the influence of momentum-dependent interactions on the collective flow of heavy-ion collisions. Over the years the model has been extensively applied to study not only heavy-ion collisions but also the properties of nuclear matter by proper modification [1,26–29]. A review analysis of the present model is presented in Refs. [1,24].

In the present work, we have studied the momentum and temperature dependence of the mean-field properties of asymmetric nuclear matter [30–52]. Efforts up to now have been devoted mostly to studying the properties of cold nuclear matter. In contrast, the motivation for the present work is to study the properties of hot asymmetric nuclear matter, especially the temperature dependence of the nuclear symmetry energy and the single-particle properties of nuclear matter.

We have employed a model with the characteristic property that the interacting part of the energy density is momentum dependent. Thus, the single-particle potentials of protons and neutrons, as well as the symmetry potential, are also momentum dependent. The isovector part of the optical potential, i.e., the symmetry potential, describes the difference between the neutron and proton single-particle potentials in neutron-rich matter. The symmetry potential is one of the basic inputs to the transport models for the collisions of

radioactive nuclei [30]. In addition, due to the momentum dependence, the temperature is expected to affect not only the kinetic part but also the interacting part of the energy density. This is important in the sense that the density dependence of the nuclear symmetry energy, influenced by temperature, has a powerful effect on the values of the proton fraction and consequently the composition of hot β-stable nuclear matter, with extensive applications in heavy-ion collisions and nuclear astrophysics.

The effective mass (EM) is one of the most fundamental properties characterizing the propagation of a nucleon in a nuclear medium. Knowledge about nucleon EM in neutron-rich matter is crucial to fully understand several properties of neutron stars. EM is determined by the derivative of the single-particle potential with respect to the momenta k for $k = k_F$. Thus, the trend of the EM is directly connected to the momentum dependence of the corresponding single-particle potential. Furthermore, the isospin splitting of the effective mass, i.e., the difference between the neutron and proton effective masses, is derived from the above model. The present study is a contribution to the theoretical study of the neutron-proton effective mass splitting, a problem that is still highly controversial within different approaches and/or using different nuclear effective interactions [8]. The above analysis indicates the necessity of applying a momentum-dependent interacting model to study the single-particle properties of hot nuclear matter.

This work is a continuation of recent articles [37,42], where the authors have employed a phenomenological nonrelativistic effective interaction first introduced in Refs. [1,26], with suitable modification concerning the isovector part of the interaction. Here, we have applied a more generalized expression of the interaction part of the energy density, with a richer parametrization and additional parameters introduced to maintain causality [1]. We have concentrated on a systematic study of the effect of the parametrization of the effective interaction on the mean-field properties of hot asymmetric nuclear matter.

This article is organized as follows. In Sec. II the model and the related formulas are discussed and analyzed. Results are reported and discussed in Sec. III, whereas Sec. IV contains a summary.

II. THE MODEL

The schematic potential model used in the present work is designed to reproduce the results of microscopic calculations of both nuclear and neutron-rich matter at zero temperature and can be extended to finite temperature [1,26]. The energy density of the asymmetric nuclear matter (ANM) is given by the relation

$$\epsilon(n_n, n_p, T) = \epsilon_{\rm kin}^n(n_n, T) + \epsilon_{\rm kin}^p(n_p, T) + V_{\rm int}(n_n, n_p, T),$$

(1)

where n_n (n_p) is the neutron (proton) density and the total baryon density is $n = n_n + n_p$. The contribution of the kinetic parts is

$$\epsilon_{\rm kin}^n(n_n, T) + \epsilon_{\rm kin}^p(n_p, T)$$
$$= 2 \int \frac{d^3k}{(2\pi)^3} \frac{\hbar^2 k^2}{2m} [f_n(n_n, k, T) + f_p(n_p, k, T)], \quad (2)$$

where f_τ, (for $\tau = n, p$) is the Fermi-Dirac distribution function with the form

$$f_\tau(n_\tau, k, T) = \left\{ 1 + \exp\left[\frac{e_\tau(n_\tau, k, T) - \mu_\tau(n_\tau, T)}{T} \right] \right\}^{-1}.$$

(3)

This distribution is inserted into the following integral to evaluate the nucleon density n_τ,

$$n_\tau = 2 \int \frac{d^3k}{(2\pi)^3} f_\tau(n_\tau, k, T).$$

(4)

In Eq. (3), $e_\tau(n_\tau, k, T)$ is the single-particle energy (SPE) having the form

$$e_\tau(n_\tau, k, T) = \frac{\hbar^2 k^2}{2m} + U_\tau(n_\tau, k, T).$$

(5)

$\mu_\tau(n_\tau, T)$ stands for the chemical potential of each species, whereas the single-particle potential $U_\tau(n_\tau, k, T)$ is obtained by the functional derivative of the interaction part of the energy density with respect to the distribution function f_τ.

Including the effect of finite-range forces between nucleons to avoid acausal behavior at high densities, the potential contribution is parameterized as follows:

$$V_{\rm int}(n_n, n_p, T) = \frac{1}{3} A n_0 \left[\frac{3}{2} - \left(\frac{1}{2} + x_0 \right) I^2 \right] u^2$$
$$+ \frac{\frac{2}{3} B n_0 \left[\frac{3}{2} - \left(\frac{1}{2} + x_3 \right) I^2 \right] u^{\sigma+1}}{1 + \frac{2}{3} B' \left[\frac{3}{2} - \left(\frac{1}{2} + x_3 \right) I^2 \right] u^{\sigma-1}}$$
$$+ u \sum_{i=1,2} \left[C_i \left(\mathcal{J}_n^i + \mathcal{J}_p^i \right) \right.$$
$$\left. + \frac{(C_i - 8Z_i)}{5} I \left(\mathcal{J}_n^i - \mathcal{J}_p^i \right) \right], \quad (6)$$

where

$$\mathcal{J}_\tau^i(n, I, T) = 2 \int \frac{d^3k}{(2\pi)^3} g(k, \Lambda_i) f_\tau.$$

(7)

In Eq. (6), $I = (n_n - n_p)/n$ and $u = n/n_0$, with n_0 denoting the equilibrium symmetric nuclear matter density $n_0 = 0.16$ fm^{-3}. The parameters A, B, σ, C_1, C_2, and B', which appear in the description of symmetric nuclear matter and the additional parameters x_0, x_3, Z_1, and Z_2 used to determine the properties of asymmetric nuclear matter, are treated as parameters constrained by empirical knowledge [1,26].

The first two terms of the right-hand side of Eq. (6) arise from local contact nuclear interactions that led to power density contributions such as in the standard Skyrme equation of state. These are assumed to be temperature independent. The third term describes the effects of finite range interactions, according to the choice of the function $g(k, \Lambda_i)$, and is the temperature-dependent part of the interaction [26]. The function, $g(k, \Lambda_i)$, may have the following forms:

(i) Case 1:

$$g_1(k, \Lambda_i) = \left[1 + \left(\frac{k}{\Lambda_i} \right)^2 \right]^{-1}. \qquad (8)$$

In this case we introduce two finite-range terms: one corresponding to a long-range attraction and the other to a short-range repulsion. The finite-range parameters are $\Lambda_1 = 1.5 k_F^0$ and $\Lambda_2 = 3 k_F^0$ and k_F^0 is the Fermi momentum at the saturation point n_0. The function $g_1(k, \Lambda_i)$ has been used extensively in previous article (see Refs. [1,26] and references therein).

(ii) Case 2:

$$g_2(k, \Lambda_i) = \left[1 - \left(\frac{k}{\Lambda_i} \right)^2 \right]. \qquad (9)$$

In this case the finite-range interactions are approximated by effective local interactions by retaining only the quadratic momentum dependence. Therefore, the energy density in Eq. (1) takes the form of Skyrme's effective interactions. Actually, as we will show later, the two functions coincide, for low value of momenta k ($k < 1$ fm^{-1}), but they exhibit different trends for high values of k.

The energy density of asymmetric nuclear matter at density n and temperature T, in good approximation, is expressed as

$$\epsilon(n, T, I) = \epsilon(n, T, I = 0) + \epsilon_{\text{sym}}(n, T, I), \qquad (10)$$

where

$$\epsilon_{\text{sym}}(n, T, I) = n I^2 E_{\text{sym}}^{\text{tot}}(n, T)$$
$$= n I^2 \left[E_{\text{sym}}^{\text{kin}}(n, T) + E_{\text{sym}}^{\text{int}}(n, T) \right]. \qquad (11)$$

In Eq. (11) the nuclear symmetry energy $E_{\text{sym}}^{\text{tot}}(n, T)$, is separated in two parts, i.e., $E_{\text{sym}}^{\text{kin}}(n, T)$ (kinetic) and $E_{\text{sym}}^{\text{int}}(n, T)$ (interaction).

From Eqs. (10) and (11) and setting $I = 1$, we obtain that the nuclear symmetry energy $E_{\text{sym}}^{\text{tot}}(n, T)$ is given by

$$E_{\text{sym}}^{\text{tot}}(n, T) = \frac{1}{n} [\epsilon(n, T, I = 1) - \epsilon(n, T, I = 0)]. \qquad (12)$$

Thus, from Eqs. (12) and (1) and a suitable choice of the parameters $x_0, x_3, Z_1,$ and Z_2, we can obtain different forms for the density dependence of the symmetry energy $E_{\text{sym}}^{\text{tot}}(n, T)$. It is well known that the need to explore different forms for $E_{\text{sym}}^{\text{tot}}(n, T)$ stems from the uncertain behavior at high density [1]. The high-density behavior of symmetry energy is the least known property of dense matter [53–55], with different nuclear models giving contradictory predictions. Thus, in relativistic mean-field (RMF) models, symmetry energy strongly increases with the density of nuclear matter [56], whereas in many realistic potential models of nuclear matter in the variational approach [34], the symmetry energy saturates and then bends over at higher densities.

Recently, the density dependence of the symmetry energy in the equation of state of isospin asymmetric nuclear matter has been studied using isoscaling of the fragment yields and the antisymmetrized molecular dynamic calculation [57]. It

was observed that the experimental data at low densities are consistent with the form of symmetry energy, $E_{\text{sym}}(u) \approx 31.6 \, u^{0.69}$, in close agreement with those predicted by the results of variational many-body calculations. In Ref. [57] it was suggested also that the heavy-ion studies favor a dependence of the form $E_{\text{sym}}(u) \approx 31.6 \, u^{\gamma}$, where $\gamma = 0.6$–1.05. This constrains the form of the density dependence of the symmetry energy at higher densities, ruling out an extremely "stiff" and "soft" dependence [57].

Additionally, by using the isospin-dependent Boltzmann-Uehling-Uhlenbeck transport model calculations, Chen *et al.* [29] also showed that a stiff density dependence of the symmetry energy parameterized as $E_{\text{sym}}(u) \approx 31.6 \, u^{1.05}$ clearly explains the isospin diffusion data [58] from NSCL-MSU (National Superconducting Cyclotron Laboratory at Michigan State University).

In the present work, because we are interested mainly in the study of thermal effects on the nuclear symmetry energy, we choose a specific form for it, enabling us to accurately reproduce the results of many other theoretical studies [59,60]. In Ref. [59] the authors carried out a systematic analysis of the nuclear symmetry energy in the formalism of the relativistic Dirac-Brueckner-Hartree-Fock approach, using the Bonn one-boson-exchange potential. In a very recent work [60], the authors applied a similar method to that in Ref. [59] for the microscopic predictions of the equation of state in asymmetric nuclear matter. In that case $E_{\text{sym}}(u)$ was obtained by employing the simple parametrization $E_{\text{sym}}(u) = C u^{\gamma}$ with $\gamma = 0.7$–1.0 and $C \approx 32$ MeV. The authors concluded that a value of γ close to 0.8 gives a reasonable description of their predictions, although the use of different functions in different density regions may be best for an optimal fit [60]. The results of Refs. [59,60] are well reproduced by parameterizing the nuclear symmetry energy according to the formula

$$E_{\text{sym}}^{\text{tot}}(n, T = 0) = \underbrace{13 u^{2/3}}_{\text{Kinetic}} + \underbrace{17 F(u)}_{\text{Interaction}}. \qquad (13)$$

For the function $F(u)$, which parametrizes the interaction part of the SE, we apply the following three different cases

$$F_1(u) = \sqrt{u}, \quad F_2(u) = u, \quad F_3(u) = \frac{2 u^2}{1 + u}. \qquad (14)$$

The parameters $x_0, x_3, Z_1,$ and Z_2 are chosen so that Eq. (12), for $T = 0$, reproduces the results of Eq. (13) for the three different forms of the function $F(u)$. In addition, the parameters $A, B, \sigma, C_1, C_2,$ and B' are determined in order that $E(n = n_0) - mc^2 = -16$ MeV, $n_0 = 0.16$ fm^{-3}, and the incompressibility to be $K = 120, 180, 240$ MeV for each of the three cases.

A. Single-particle potentials

The single-particle energy e_τ, obtained by the functional derivative of the energy density [Eq. (1)] with respect to the distribution function f_τ, is written as

$$e_\tau(n, I, k, T) = \frac{\hbar^2 k^2}{2m} + U_\tau(n, I, k, T). \qquad (15)$$

The single-particle energy e_τ consists of a kinetic part and an interaction one $U_\tau(n, I, k, T)$, which depends explicitly on density, momentum, isospin asymmetry, and temperature as expected from an interaction term.

The single-particle potential $U_\tau(n, I, k, T)$ (protons or neutrons), obtained from the functional derivative of the interaction part of the energy density [Eq. (6)] with respect to the distribution function f_τ, has the general form

$$U_\tau(n, I, k, T) = U_\tau^A(n, I) + U_\tau^B(n, I) + U_\tau^{\mathrm{MD}}(n, I, k, T). \tag{16}$$

The first two terms are momentum independent, whereas the third one describes the momentum dependence of the single-particle potential. The three terms have the following forms

$$U_\tau^A(n, I) = Au \mp \frac{2}{3} A \left(\frac{1}{2} + x_0 \right) uI, \tag{17}$$

$$U_n^B(n, I) = \frac{U_\tau^{B1}(n, I) U_\tau^{B2}(n, I) - U_\tau^{B3}(n, I) U_\tau^{B4}(n, I)}{\left[U_\tau^{B2}(n, I) \right]^2}, \tag{18}$$

with

$$U_\tau^{B1}(n, I) = B(\sigma + 1)u^\sigma \mp \frac{4}{3} B \left(\frac{1}{2} + x_3 \right) u^\sigma I$$
$$+ \frac{2}{3} B(1 - \sigma) \left(\frac{1}{2} + x_3 \right) u^\sigma I^2,$$

$$U_\tau^{B2}(n, I) = 1 + \frac{2}{3} B' \left[\frac{3}{2} - \left(\frac{1}{2} + x_3 \right) I^2 \right] u^{\sigma-1},$$

$$U_\tau^{B3}(n, I) = \frac{B'}{n_0} (\sigma - 1) u^{\sigma-2} \mp \frac{4}{3} \frac{B'}{n_0} \left(\frac{1}{2} + x_3 \right) u^{\sigma-2} I$$
$$+ \frac{2}{3} \frac{B'}{n_0} (3 - \sigma) \left(\frac{1}{2} + x_3 \right) u^{\sigma-2} I^2,$$

$$U_\tau^{B4}(n, I) = \frac{2}{3} B n_0 \left[\frac{3}{2} - \left(\frac{1}{2} + x_3 \right) I^2 \right] u^{\sigma+1} \tag{19}$$

and

$$U_\tau^{\mathrm{MD}}(n, I, k, T)$$
$$= \frac{4}{5} \frac{1}{n_0} \sum_{i=1,2} \left[\frac{1}{2} (3C_i - 4Z_i) \mathcal{J}_\tau^i + (C_i + 2Z_i) \mathcal{J}_{\tau'}^i \right]$$
$$+ u \sum_{i=1,2} \left[\left(C_i \pm \frac{C_i - 8Z_i}{5} I \right) g(k, \Lambda_i) \right]. \tag{20}$$

The subscripts in the integrals are $\tau \neq \tau'$; the upper signs stand for neutrons, whereas the lower ones stand for protons. An advantage of the present model is that for $T = 0$, the term $U_\tau^{\mathrm{MD}}(n, I, k, T)$, as well as all the quantities can be derived in analytical forms.

It is of interest to see that the single-particle potentials are separated into two parts. The first one, $U_\tau^A(n, I) + U_\tau^B(n, I)$,

is a function only of the baryon density n and the isospin asymmetry parameter I. The second one, $U_\tau^{\mathrm{MD}}(n, I, k, T)$, has an additional dependence on T and k. Actually, $U_\tau^{\mathrm{MD}}(n, I, k, T)$ is mainly responsible for the trend of the effective mass and also the effective mass splitting. Additionally, it is connected with the effect of the temperature on the interacting part of the energy density. It is also worthwhile noticing the direct correlation between the regulator function $g(k, \Lambda_i)$ and $U_\tau^{\mathrm{MD}}(n, I, k, T)$. Thus, the choice of the function $g(k, \Lambda_i)$ plays an important role for the single-particle properties of hot nuclear matter, but one expects it to also be significant for the bulk properties of nuclear matter.

B. Nuclear symmetry potential

The nuclear symmetry potential (NSP) refers to the isovector part of the nucleon mean-field potential in isospin asymmetric nuclear matter, which in hot nuclear matter can also depend on the temperature. Most of the studies concerning the NSP have been carried out for zero temperature, whereas the temperature dependence of the NSP so far has received little theoretical attention [8]. The NSP potential, describes the difference between the neutron and proton single-particle potentials in neutron-rich matter and has the form

$$U_{\mathrm{sym}}(n, I, k, T) = \frac{U_n(n, I, k, T) - U_p(n, I, k, T)}{2I}. \tag{21}$$

Various theoretical models have been applied to study the symmetry potential. Most of them predict a symmetry potential decreasing with increasing nucleon momentum. However, some nuclear models that employed effective interaction, predict an opposite behavior [8].

A systematic analysis of a large number of nucleon-nucleus scattering experiments and (p, n) charge-exchange reactions at beam energies up to 100 MeV has shown that the data can be very well described by the parametrization

$$U_{\mathrm{sym}}(E_{\mathrm{kin}}) = a - b E_{\mathrm{kin}}, \tag{22}$$

with $a \approx 22$–34 MeV and $b = 0.1$–0.2. Actually, the uncertainties for both parameters a and b are large. As pointed out in Ref. [45], the old analysis of Lane [61] is consistent with a decreasing trend of the potential as function of k, whereas a more recent analysis based on Dirac phenomenology [62] leads to the opposite conclusions.

To clarify the effects of the momentum dependence on the NSP, it is easy to show, by applying Eqs. (16)–(20), that $U_{\mathrm{sym}}(n, I, k, T)$, at zero temperature is

$$U_{\mathrm{sym}}(n, I, k) = U_{\mathrm{sym}}^{\mathrm{MIP}}(n, I) + U_{\mathrm{sym}}^{\mathrm{MDP}}(n, k). \tag{23}$$

In Eq. (23), $U_{\mathrm{sym}}^{\mathrm{MIP}}(n, I)$ is momentum independent, whereas the momentum-dependent part $U_{\mathrm{sym}}^{\mathrm{MDP}}(n, k)$ is written as

$$U_{\mathrm{sym}}^{\mathrm{MDP}}(n, k) = \frac{u}{5} \sum_{i=1,2} (C_i - 8Z_i) g(k, \Lambda_i). \tag{24}$$

From Eq. (24) it is obvious that the behavior of $U_{\mathrm{sym}}(n, k)$ as a function of k is defined from the values of the parameters C_i and Z_i, as well as from the function $g(k, \Lambda_i)$. In fact, the regulator function $g(k, \Lambda_i)$ specifies the trend of the slope. Thus, it is interesting to study the effect of the parametrization,

including the function $F(u)$, and the contribution of the choice of a specific function $g(k, \Lambda_i)$ on the properties of the NSP for both cold and hot nuclear matter.

C. Effective mass

The nucleon effective mass is one of the most important single-particle properties of nuclear matter. It characterizes the momentum dependence of the single-particle potential of a nucleon and consequently the quasiparticle properties of a nucleon inside a strongly interacting medium such as the nuclear matter. Moreover, the effective mass describes to leading order the effects related to the nonlocality of the underlying nuclear effective interaction and the Pauli exchange effects in many-fermion systems [37,45,63].

The effective mass $m_\tau^*(k)$, is determined by the momentum-dependent single nucleon potential via

$$\frac{m_\tau^*(n, I, k)}{m_\tau} = \left[1 + \frac{m_\tau}{\hbar^2 k} \frac{dU_\tau(n, I, k, T)}{dk}\right]^{-1}. \quad (25)$$

According to Eq. (25), $m_\tau^*(n, I, k)$ generally depends on the baryon density, the isospin asymmetry, and the momentum of the nucleon. In the present model m_τ^* is independent of T.

An evaluation of m_τ^* mass at the Fermi momentum $k = k_F$, employing Eq. (25), yields the Landau effective mass. An advantage of the present model is that by applying Eq. (16), we get m_τ^* in analytical form, i.e.,

$$\frac{m_\tau^*(n, I)}{m_\tau} = \left[1 + u\frac{m_\tau}{\hbar^2 k_F} \sum_{i=1,2} \left(C_i \pm \frac{C_i - 8Z_i}{5}I\right)\right.$$
$$\left. \times \frac{dg(k, \Lambda_i)}{dk}\Big|_{k=k_F}\right]^{-1}. \quad (26)$$

Equation (26) exhibits the dependence of the effective mass on the values of the parameters C_i, Z_i, and Λ_i as well as on the derivative of the regulator function $g(k, \Lambda_i)$. In particular, for the two cases of the function $g(k, \Lambda_i)$ [given in Eqs. (8), and (9)], we get, respectively, for the effective masses

$$\frac{m_\tau^*(n, I)}{m_\tau} = \left[1 - \frac{2um_\tau}{\hbar^2} \sum_{i=1,2} \frac{1}{\Lambda_i^2} \frac{\left(C_i \pm \frac{C_i - 8Z_i}{5}I\right)}{\left[1 + \left(\frac{k_F^0}{\Lambda_i}\right)^2 [(1 \pm I)u]^{2/3}\right]^2}\right]^{-1}, \qquad \text{Case 1} \quad (27)$$

$$\frac{m_\tau^*(n, I)}{m_\tau} = \left[1 - \frac{2um_\tau}{\hbar^2} \sum_{i=1,2} \frac{1}{\Lambda_i^2} \left(C_i \pm \frac{C_i - 8Z_i}{5}I\right)\right]^{-1}. \qquad \text{Case 2} \quad (28)$$

The meaning of Eqs. (27) and (28) is clear. First, the Landau effective mass for protons and neutrons depends on the parameters C_i and Z_i, where C_i is connected with the saturation properties of nuclear matter and Z_i with the density dependence of the nuclear symmetry energy. Second, m_τ^* depends on the baryon density via the variable u, as well as on the isospin parameter I. Finally, there is also a direct dependence of m_τ^* on the regulator function $g(k, \Lambda_i)$ via the parameters Λ_i. Hence, one can conclude that the values of the effective mass are reflected on the specific properties of the applied nuclear models. This enables us to carry out a systematic study of the properties of m_τ^* by applying the parametrization of the present model.

III. RESULTS AND DISCUSSION

We have studied thermal and momentum-dependent effects on the properties of hot asymmetric nuclear matter including mean field potentials (proton, neutron and symmetry) as well as the effective mass, by applying a momentum-dependent effective interaction. The parametrization of the model can be found in Table 1 and Table 2 of Ref. [1].

In particular, we have studied two general cases. In the first one (called g_1) the momentum regulator function $g(k, \Lambda_i)$ is given by equation (8). In this case, the quantity $\mathcal{J}_\tau^i$ defined by

Eq. (7), at $T = 0$, takes the form

$$\mathcal{J}_\tau^{i(g_1)}(n, I) = \frac{3}{2}n_0 \left(\frac{\Lambda_i}{k_F^0}\right)^3 \left\{\frac{[(1 \pm I)u]^{1/3}}{\frac{\Lambda_i}{k_F^0}}\right.$$
$$\left. - \tan^{-1}\frac{[(1 \pm I)u]^{1/3}}{\frac{\Lambda_i}{k_F^0}}\right\}, \quad (29)$$

where the upper signs refer to neutrons and the lower ones to protons.

In the second case (called g_2) the momentum regulator function $g(k, \Lambda_i)$ is given by Eq. (9). Here, the finite-range interactions are approximated as effective local interactions by retaining only the quadratic momentum dependence [1,14]. In this case, the energy density takes the form of Skyrme's effective interaction. At $T = 0$ the quantity $\mathcal{J}_\tau^i$ is

$$\mathcal{J}_\tau^{i(g_2)}(n, I) = \frac{9}{2}n_0 [(1 \pm I)u]^{1/3} \left\{1 - \frac{3}{5}\frac{[(1 \pm I)u]^{2/3}}{\left(\frac{\Lambda_i}{k_F^0}\right)^2}\right\}. \quad (30)$$

The parameters A, B, σ, C_1, C_2, and B' (a small parameter introduced to maintain causality) are determined from
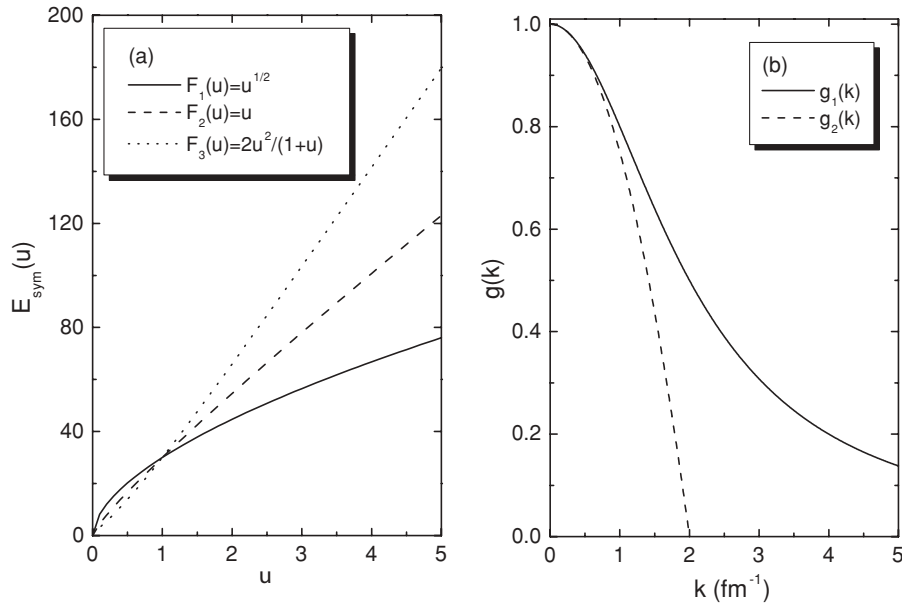
FIG. 1. (a) The nuclear symmetry energy as a function of $u = n/n_0$ for three different parametrizations of the function $F(u)$ given by Eq. (14). (b) The regulator momentum function $g(k, \Lambda)$ for the two cases, given by Eqs. (8) and (9), applied in the present work. For more details see text.

constraints provided by the empirical properties of symmetric nuclear matter at the equilibrium density $n_0 = 0.16$ fm^{-3}. With the appropriate choice of the parameters, it is possible to parametrically vary the nuclear incompressibility K so the dependence on the stiffness of the equation of state may be explored. In the same way, by choosing the appropriate parameters x_0, x_3, Z_1, and Z_2, it is possible to obtain different forms for the density dependence of the nuclear symmetry energy [1,26].

Figure 1(a) displays the behavior of the NSE as a function of the ratio $u = n/n_0$ for the three different parametrizations of the function $F(u)$ (relation [14]). The function $F_3(u)$ leads

to a stiffer nuclear symmetry energy dependence on the density, whereas the function $F_1(u)$ leads to a softer one. It is worthwhile pointing out that the above parametrization of the interacting part of the nuclear symmetry energy is extensively used for the study of neutron star properties [1,26], as well as for the study of the collisions of neutron-rich heavy ions with intermediate energies [32,64]. For a very recent review of the applications of the proposed momentum-dependent effective interaction model and the specific parametrization of it, see Ref. [65] (and references therein). The aim of the above simple parametrization is to reproduce the nuclear symmetry energy originating from various theoretical calculations and/or
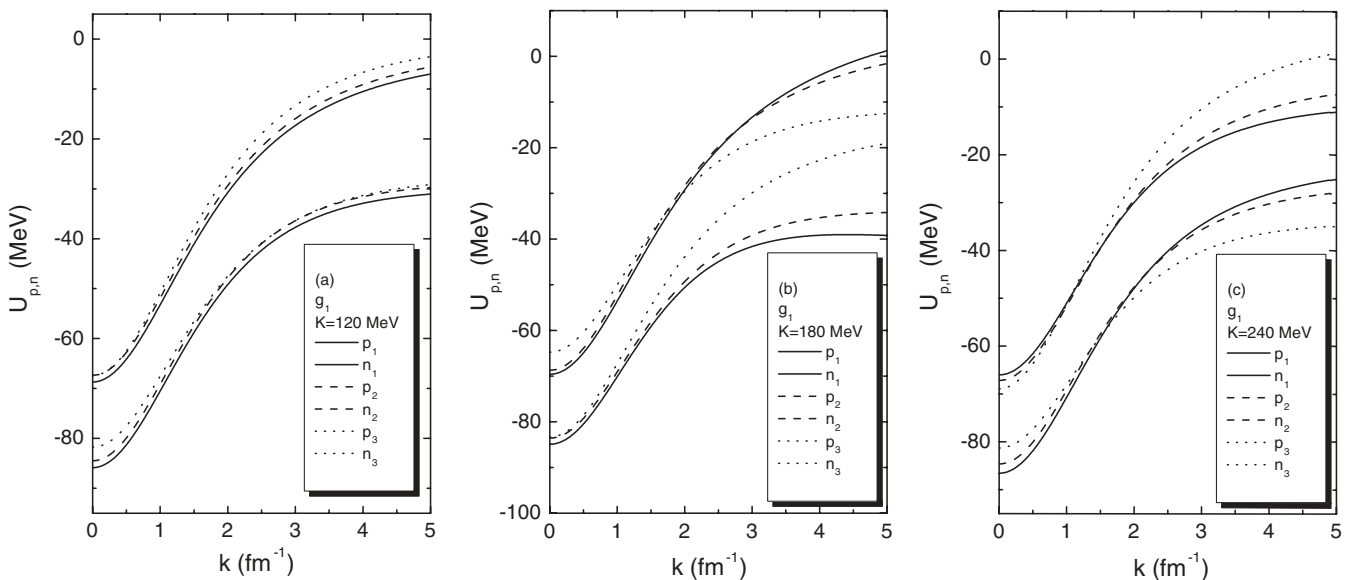

FIG. 2. The proton and neutron single-particle potentials (the upper curves corresponds to U_n, whereas the lower one corresponds to U_p) for the case g_1 and for three different vales of the incompressibility K (at the saturation density n_0). In each figure we display U_p and U_n for three different forms of the nuclear symmetry energy (named 1, 2, and 3, respectively).
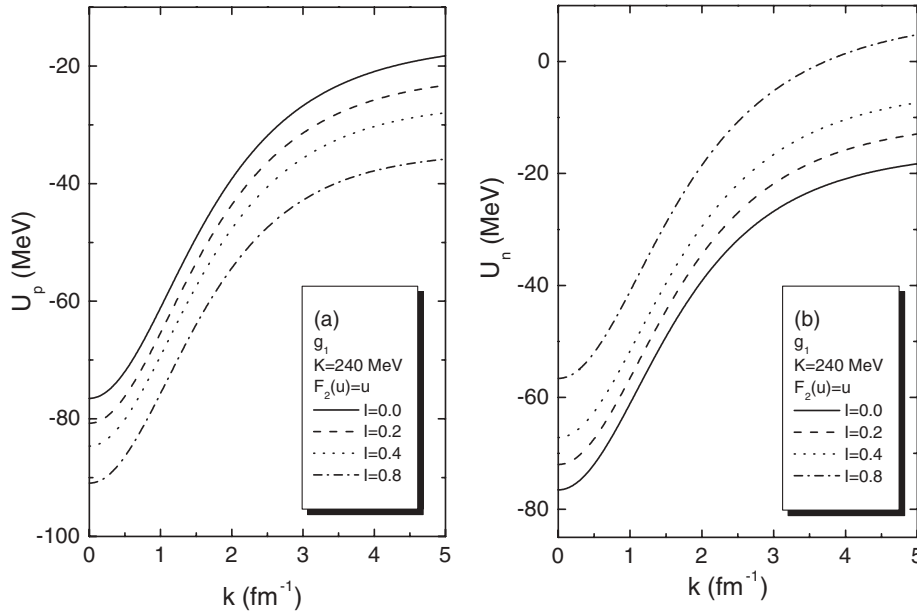
FIG. 3. U_p and U_n, in case g_1 and for $K = 240$ MeV and $F_2(u) = u$ versus k and for various values of the asymmetry parameter $I = (n_n - n_p)/n$.

experimental predictions and also to be able to cover the possible range of the nuclear symmetry energy dependence on the density.

In Fig. 1(b) we plot the regulator momentum function $g(k, \Lambda_1)$ for the two cases applied in the present work. The most striking feature of the two curves is the fact that for low values of the momenta k, the two cases coincide, but for higher values of k they have completely different behavior. The motivation for applying these two different parametrizations for the momentum part of the interaction is to investigate in greater detail the momentum dependence effects on the mean-field properties of hot asymmetric matter.

The nuclear symmetry potential, pertaining to the isovector part of the nucleon mean-field potential of a nucleon in nuclear matter, also depends on the momentum of the nucleon. To see the temperature and momentum effects on the nuclear symmetry potential, we first study the above effects on the

nucleon single-particle potentials in hot asymmetric nuclear matter.

In Fig. 2 we present the behavior of the proton and neutron single-particle potentials for the case g_1 and three different values of the incompressibility K. The calculations are performed at the saturation density n_0. In each figure we display U_p and U_n for three different forms of the symmetry energy [named 1, 2, and 3, respectively, see Eq. (14)]. It is noted that in case 3, for $K = 180$ MeV and for high values of k, U_p, and U_n obtain comparable values. As we will see later, this affects the behavior of NSP. A feature of Fig. 2 is the effect of K on the values of the SPP for high values of k. Thus, for small values of k in the three cases, both for protons and neutrons, lead to similar values for the SPP, whereas for high values of k, there is an obvious splitting of the values of SPP, which shows a monotonic increase with K.
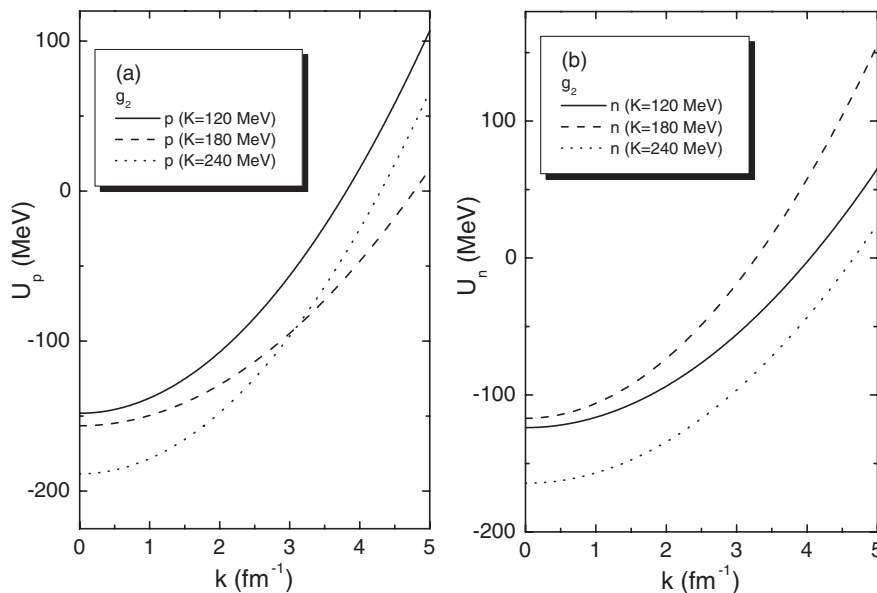

FIG. 4. U_p (left) and U_n (right) for the case g_2 and for three different values of K (at the saturation density n_0).
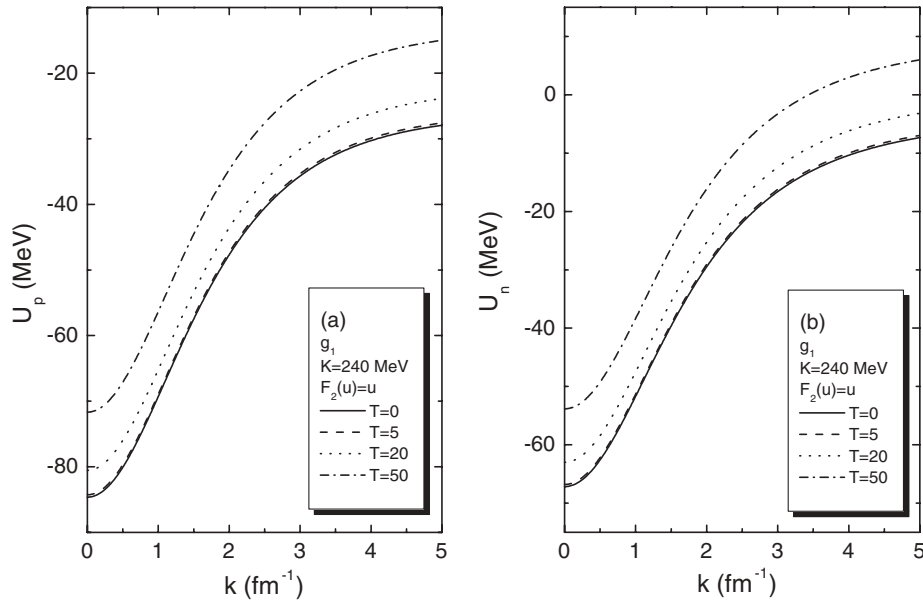
FIG. 5. U_p and U_n, in case g_1 and for $K = 240$ and $F_2(u) = u$ as a function of temperature T (in MeV) (at the saturation density n_0).

Figure 3 displays the trend of U_p and U_n, in case g_1, for $K = 240$ and $F_2(u) = u$ as a function of the asymmetry parameter $I = (n_n - n_p)/n$. The meaning of the trend is very clear. The increase of the isospin asymmetry parameter I leads to a more attractive U_p and also more repulsive U_n. Similar behavior is found in the other cases as well.

In Fig. 4 we plot $U_{p,n}$ for the case g_2 and for the three different values of K. The competitive behavior of U_p and U_n, both for low and high values, is clearly reflected in the behavior of U_{sym} as indicated later in Fig. 7.

The temperature effects on U_p, U_n are shown in Fig. 5. As expected, the increase of T leads to a corresponding increase of the values of U_p and U_n. The effects are more pronounced for $T > 5$ MeV. The temperature effect on U_p, U_n has a significant influence on the temperature depen-

dence of the nuclear symmetry energy as found in previous works [8,21].

Most of the theoretical models predict a decreasing symmetry potential with increasing nucleon momentum, albeit at different rates, whereas a few nuclear effective interactions used in some models show opposite behavior. In the present work we try to clarify the above controversial results by applying a systematic study of U_{sym}. In Fig. 6, we plot the nuclear symmetry potential $U_{sym} = (U_n - U_p)/2I$ as a function of the nucleon kinetic energy E_{kin} in case g_1, for three values of K and in each case for three different choices of $F(u)$. In the present work, we apply $I = 0.4$ in the calculation of U_{sym} and as pointed out also in [8,45], U_{sym} is almost independent of the asymmetry parameter I but depends strongly on density and momentum. It is of interest to see
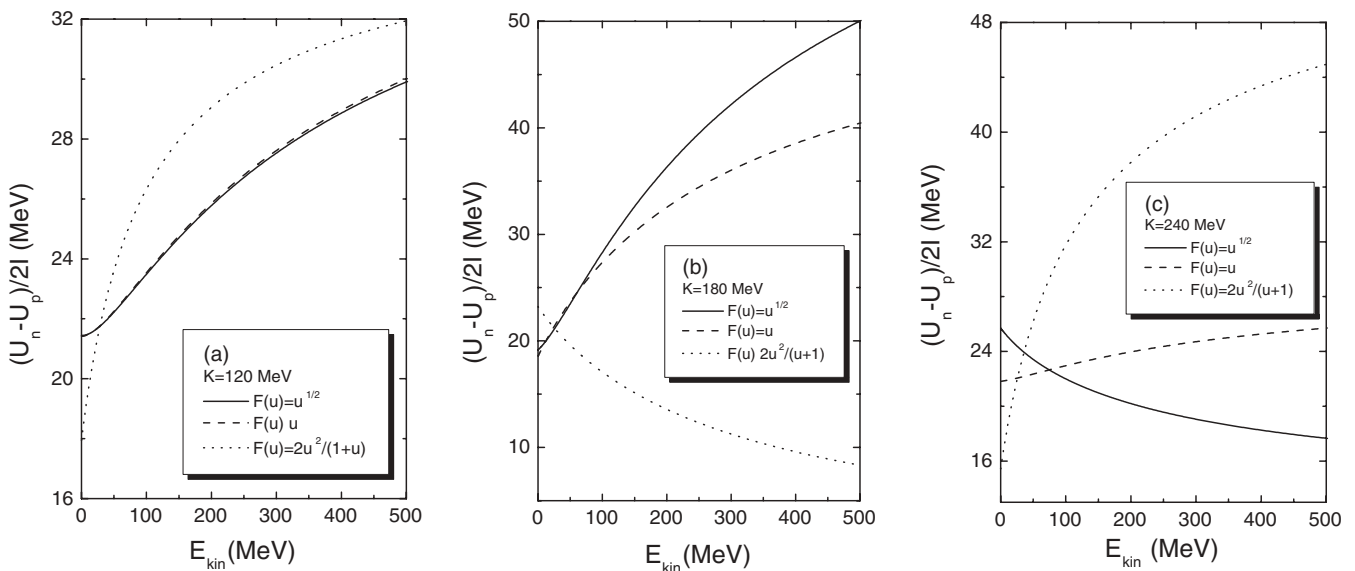

FIG. 6. The nuclear symmetry potential $U_{sym} = (U_n - U_p)/2I$ versus the nucleon kinetic energy E_{kin} in case g_1, for three values of K and in each case for three different choices of $F(u)$ (at the saturation density n_0).
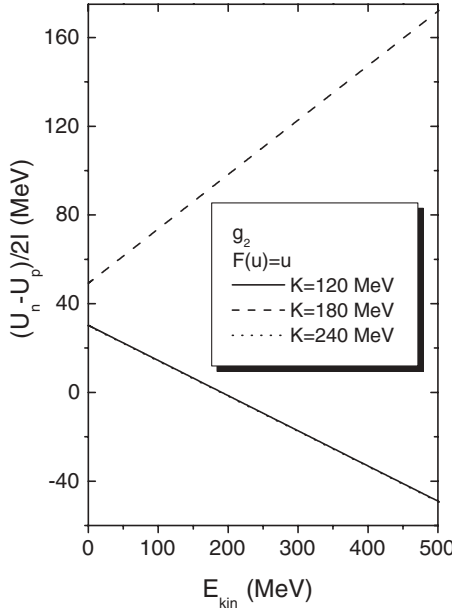
FIG. 7. $U_{\text{sym}} = (U_n - U_p)/2I$ versus E_{kin} in case g_2, for three values of K (the cases $K = 120$ MeV and $K = 240$ MeV are coincide) (at the saturation density n_0).

FIG. 8. $U_{\text{sym}} = (U_n - U_p)/2I$ versus E_{kin} for the three cases (at the saturation density n_0), which decreases with increasing of nucleon momentum, in comparison with U_{sym} constrained by the experimental data. For more details see text.

that for the nine, in total, different cases, only in two of them does U_{sym} decrease with increasing nucleon momentum [for $K = 180$ MeV and $F_3(u) = 2u^2/(u + 1)$ and for $K = 240$ MeV and $F(u) = u^{1/2}$]. This trend is in agreement with experiment, which is well reproduced using the empirical relation (22). In the remaining seven cases, U_{sym} increases with increasing nucleon momentum. In addition, from Fig. 6 it is concluded that the energy dependence of U_{sym} is sensitive to the incompressibility K.

It is worth noticing that the nuclear symmetry potentials differ from the nuclear symmetry energy as the latter involves the integration of the isospin-dependent mean-field potential of a nucleon over its momentum [8]. However, it is of interest to study the effect of the potential part of $E_{\text{sym}}(u)$ on the momentum and density dependence of U_{sym}. Figure 6 demonstrates the strong dependence of U_{sym} on the function $F(u)$. It seems that by applying the functions $F(u) = u^{1/2}$ and $F(u) = u$ we receive similar results only for low values of E_{kin} (except for $K = 120$ MeV where a similar trend is taken also for higher values of E_{kin}). The case with $F(u) = 2u^2/(u + 1)$, which introduces a much stiffer density dependence E_{sym}, leads to different results even for low values of momenta. To sum up, the density dependence of E_{sym} is well reflected on the momentum dependence of U_{sym}, so it is expected that models with different density dependence in the nuclear symmetry energy may predict different energy dependence of U_{sym}.

In Fig. 7 we also plot U_{sym} as a function of E_{kin}, for the case g_2. In fact, the trends for $K = 120$ MeV and $K = 240$ MeV coincide, and U_{sym} exhibits a negative slope, whereas for $K = 180$ MeV the slope of U_{sym} is positive.

The key quantity to explain the trend of U_{sym} as a function of E_{kin} is expression (24). For this expression we conclude that the behavior of $U_{\text{sym}}(n, k)$ as a function of k is defined from the values of the parameters C_i and Z_i as well as from the
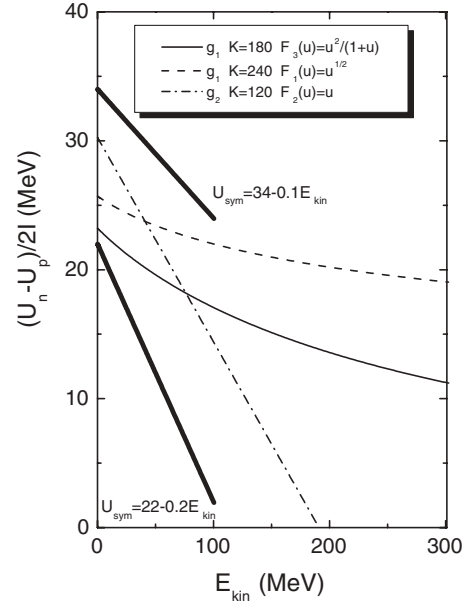
function $g(k, \Lambda_i)$. Both the parameters C_i and Z_i are related to the strength of the momentum dependence. In addition, C_i is fixed also to reproduce the properties of symmetric nuclear matter at the saturation point, while Z_i is set to fix the density dependence of the symmetry energy. The regulator function $g(k, \Lambda_i)$ mainly affects the trend of the slope of U_{sym}. In particular, in case g_2, after some algebra, the expression (24) can be written as

$$U_{\text{sym}}^{\text{MDP}}(n, k) = U_{\text{sym}}^{MI}(n, C_i, Z_i) - \mathcal{D}_1 E_{\text{kin}} u \sum_{i=1,2} \frac{(C_i - 8Z_i)}{\Lambda_i^2},$$
(31)

where $\mathcal{D}_1$ is a constant. Equation (31) establishes a linear relation between U_{sym} and E_{kin}, in case g_2, as indicated in Fig. 9.

In case g_1 for low values of k, a similar relation as (31) holds. Accordingly, for high values of k we find

$$U_{\text{sym}}^{\text{MDP}}(n, k) \simeq \frac{\mathcal{D}_2}{E_{\text{kin}}} u \sum_{i=1,2} (C_i - 8Z_i) \Lambda_i^2,$$
(32)

where $\mathcal{D}_2$ is a constant.

From the above analysis it is clear that the behavior of U_{sym} depends on the specific values of the parameters C_i, Z_i, and Λ_i and also on combinations of them. In particular, the values of the parameters define the sign of the slope (positive or negative) and the regulator function $g(k, \Lambda_i)$ defines the trend of the slope. Thus, the role of the regulator function $g(k, \Lambda_i)$ is of importance, concerning the momentum-dependent behavior of the proton and neutron single-particle potential, as well as the symmetry potential. In view of the above comment it may be interesting to explore other choices for the regulator function as those used in Ref. [66]. Such work is in progress.
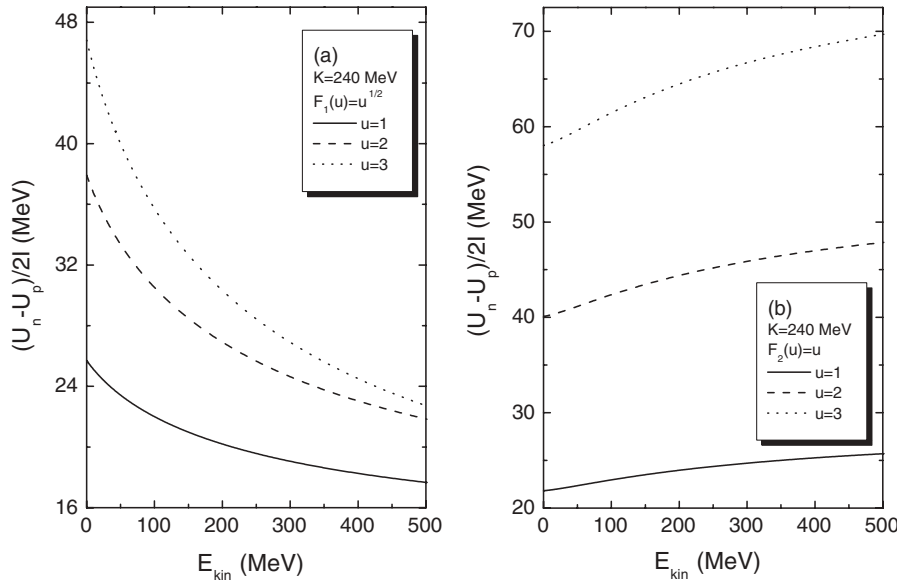
FIG. 9. $U_{\text{sym}} = (U_n - U_p)/2I$ versus E_{kin} in case g_1, for $K = 240$ MeV for three different values of u (a) for $F_1(u) = u^{1/2}$ and (b) for $F_2(u) = u$.

It is worth noting that according to Fig. 7, U_{sym} is strongly related to the density dependence of the nuclear symmetry energy and the total parametrization of the interaction energy density part, i.e., for various values of the incompressibility K. The three cases where U_{sym} is a decreasing function of nucleon momentum are shown in Fig. 8 and compared with the phenomenological expression (22). In Fig. 9 we plot U_{sym} as a function of E_{kin} for the nuclear symmetry energy parametrization $F_1(u) = u^{1/2}$ and $F_2(u) = u$ and for three different values of u. In both cases, U_{sym}, exhibits strong density-dependent behavior. In particular, there is a monotonic increase of U_{sym} as function of the nucleon density.

Special effort has been devoted to the study of the thermal effects on U_{sym}. So far, that problem has received little theoretical attention [8]. Temperature influences the first term

of the right-hand side of Eq. (23), i.e., $U_{\text{sym}}^{\text{MIP}}(n, I)$. The thermal effects on U_{sym} are displayed in Fig. 10. In the first case [Fig. 10(a)] an increase of T leads to decreasing values of U_{sym}, whereas the inverse behavior is seen in the second case [Fig. 10(b)]. However, in both cases thermal effects do play a role, especially for $T > 5$. Temperature does not change the trend, but only slightly affects the values of U_{sym} depending on E_{kin}.

Another quantity of interest, which can be easily calculated, is the isoscalar potential. Several decades ago, it was already pointed out that the quantity $(U_n + U_p)/2$, which is obviously the single-nucleon potential in absence of asymmetry, should be a reasonable approximation to the isoscalar part of the optical potential. The momentum dependence of $(U_n + U_p)/2$ is important for extracting information about the symmetric matter equation of state [41]. Now, to check the validity of the
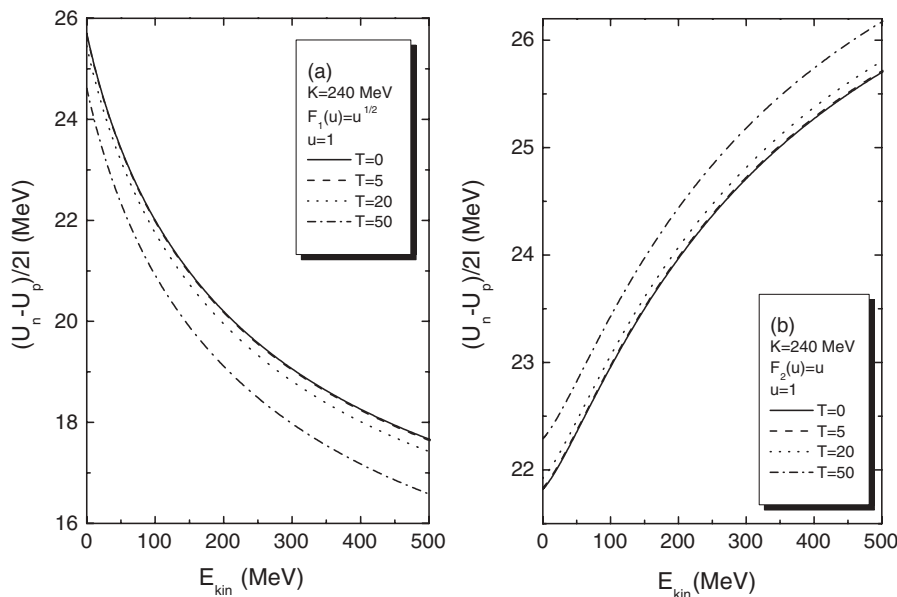

FIG. 10. $U_{\text{sym}} = (U_n - U_p)/2I$ versus E_{kin} in case g_1, for $K = 240$ MeV for various values of T (in MeV) (a) for $F_1(u) = u^{1/2}$ and (b) for $F_2(u) = u$.
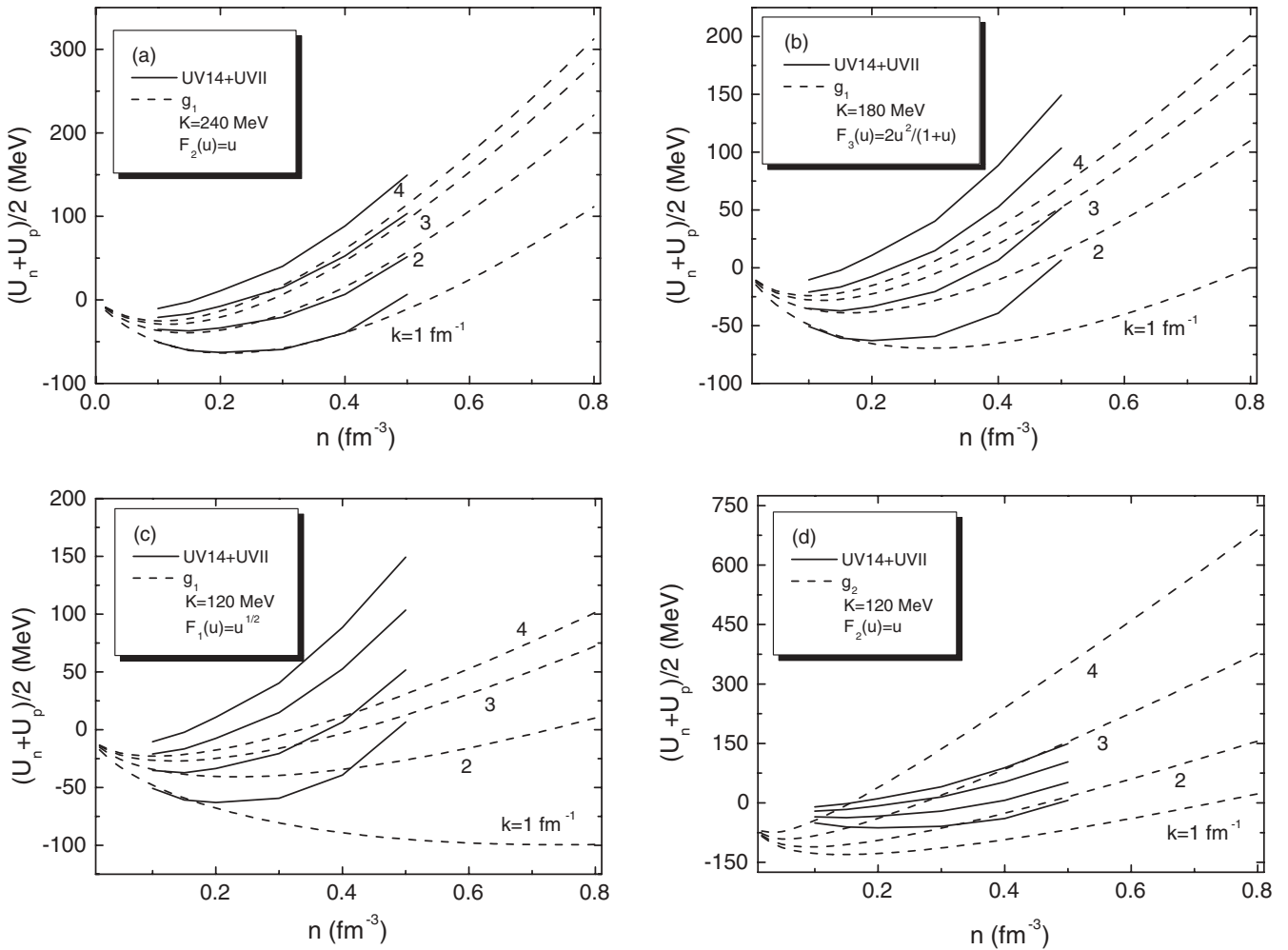
FIG. 11. The isoscalar potential $(U_n + U_p)/2$, as a function of baryon density, at the four values of the momenta k, for four different cases, in comparison with the variational many-body calculations (UV14 + UVII).

model parameters this is customary and a more stringent test to compare the isoscalar potentials, as calculated in the present work, with the variational many-body (VMB) predictions by Wiringa [34,37].

In Fig. 11 we plot the isoscalar potential at the four values of momenta k ($k = 1, 2, 3, 4$ fm^{-1}) for four different cases. The results of the present work compared with those (named UV14 + UVII) predicted by Wiringa [34]. In Fig. 11(a) indicated that for the specific case, the predictions of the present work are in very good agreement with the VMB predictions up to about $k = 3$ fm^{-1}. In a second case, presented in Fig. 11(b), there is agreement only for low values of the density and for momenta k. There is obvious disagreement for the predictions presented in Figs. 11(c) and 11(d). From the above analysis it is concluded that by suitable choice of the model parameters, we are able to reproduce and/or be consistent with the predictions of other microscopic many-body calculations or experimental constraints. This is an advantage of the present model that is flexible enough to reproduce predictions of many other theoretical models.

The Landau effective mass splitting is shown in Fig. 12, where the effective masses of proton and neutron are displayed as functions of the asymmetry parameter I for all cases corresponding to g_1. For all cases, m_p^* is a decreasing function of I, whereas m_n^* is an increasing function of I. The only exception is the case for $K = 240$ MeV with $F_3(u) = 2u^2/(u + 1)$, where m_n^* is a decreasing function of I. In every case the isospin mass splitting $(m_n^* - m_p^*)$ is positive and is directly dependent on the incompressibility K and the parametrization function $F(u)$.

In the present work, we also address the problem that arises when the effective mass splitting directly affects the energy dependence of the symmetry potential [32]. We found that in the framework of the proposed model and for the regulator function g_1, all the cases lead to a positive splitting but the slope of the U_{sym} may be positive or negative. So, it is concluded that the trend of U_{sym}, by applying the present parametrization, does not directly connect to the effective mass splitting. Nonetheless, we found that there is a correlation between U_{sym} and $m_n^* - m_p^*$ originated from the density dependence of E_{sym}. More precisely, the cases with $F(u) = u^{1/2}$ and $F(u) = u$ that
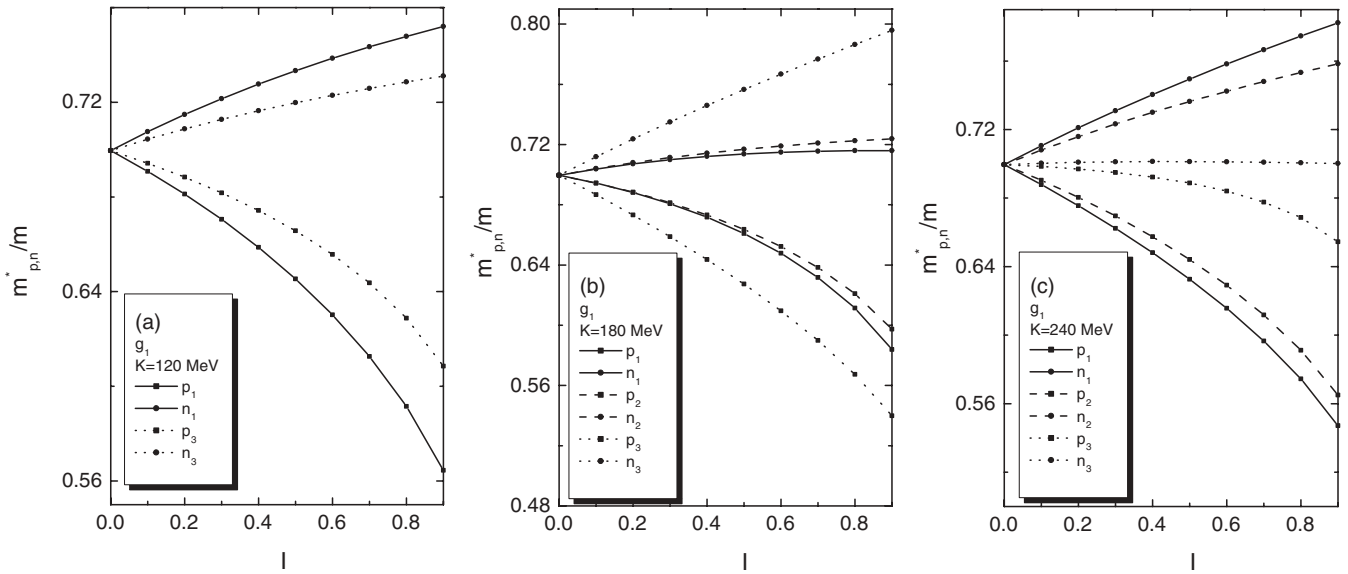
FIG. 12. The effective mass of proton and neutron as a function of the asymmetry parameter I for all the cases corresponding to g_1 (at the saturation density n_0).

lead to much closer values for U_{sym} also lead to a similar value of $m_n^* - m_p^*$ as is displayed in Figs. 12 and 13.

To illustrate further the dependence of the effective mass on the asymmetry parameter I and to find the quantitative characteristic of this dependence, the values of m_τ^*/m for various values of I have been derived with the least-squares fit method and found to take the general form

$$\frac{m_\tau^*(I)}{m} \simeq c_0 + c_1 I + c_2 I^2. \tag{33}$$

The parameters c_i depend on the model parameters C_i, Z_i, Λ_i and they are different for each case. Specifically,

for low values of I it is obvious that linear relations between m_τ^*/m and I is hold (see also Fig. 12). The splitting of effective masses, according to Eq. (33), is well approximated by

$$\Delta m^*(I) = m_n^*(I) - m_p^*(I) \simeq d_1 I + d_2 I^2, \tag{34}$$

where the parameters d_i also depend on the model parameters C_i, Z_i, Λ_i. For low values of I, the linear relation $\Delta m^*(I) \approx d_1 I$ holds. The effective mass as a function of u is indicated in Fig. 13. In all cases the effective mass splitting $(m_n^* - m_p^*)$ is positive.

In Fig. 14(a) the effective mass, for the case g_2, is displayed. The splitting $(m_n^* - m_p^*)$ is positive for the case with
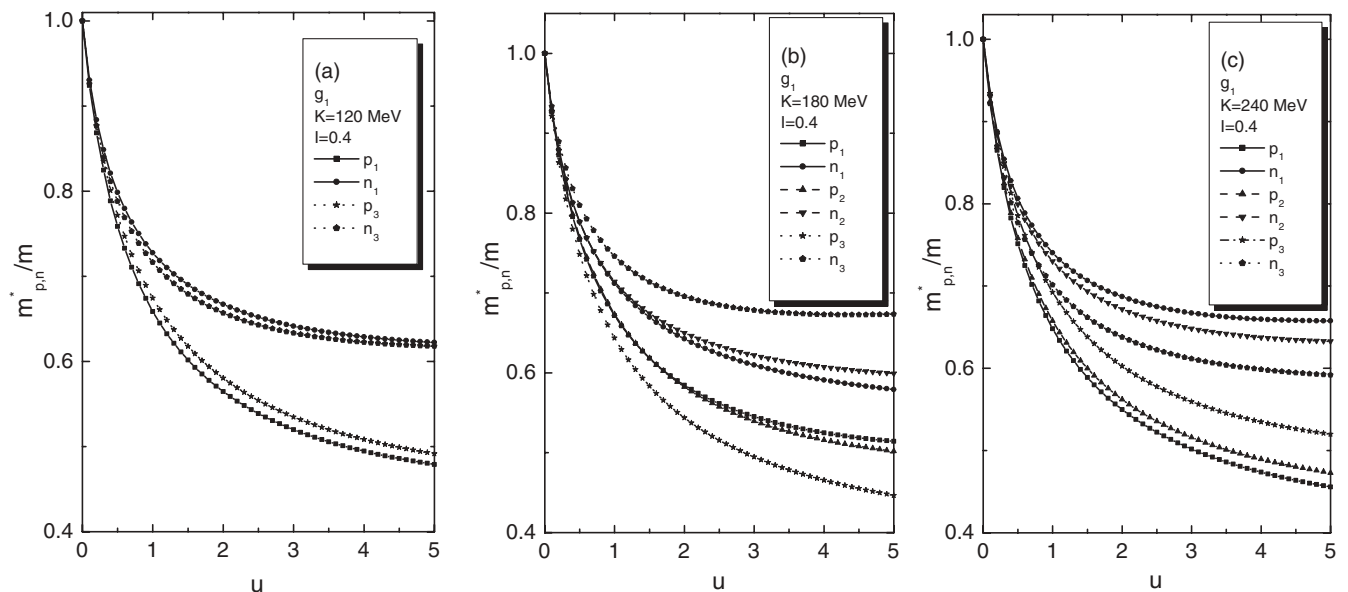

FIG. 13. The effective mass of proton and neutron versus u for all the cases corresponding to g_1.
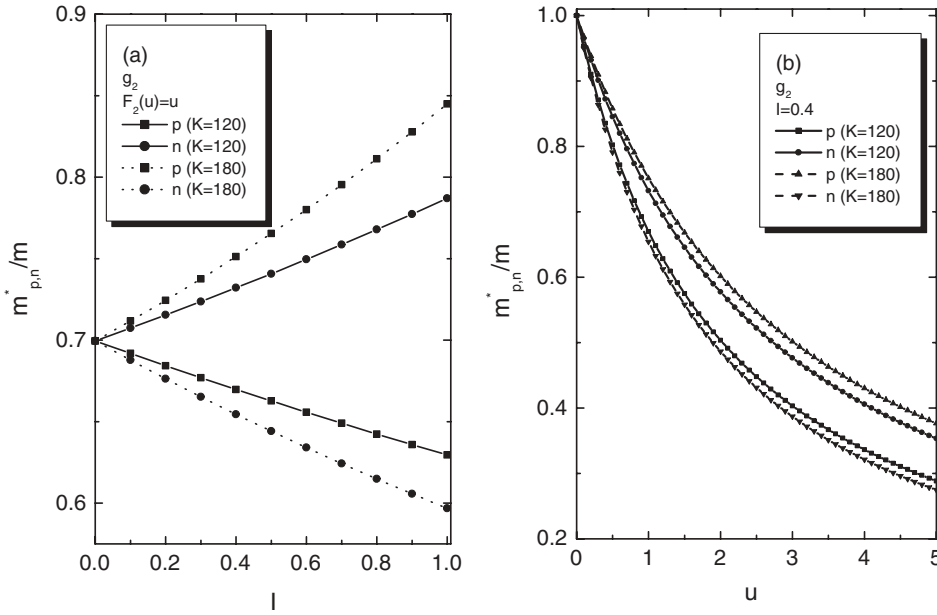
FIG. 14. (a) The effective masses of proton and neutron versus I for two cases corresponding to g_2. (b) The effective masses of proton and neutron versus u for two cases corresponding to g_2.

$K = 120$ MeV (and also for $K = 240$ MeV) and negative for $K = 180$ MeV. Thus, one can conclude by also comparing with the case g_1, that the regulator function $g(k, \Lambda_i)$ can have a dramatic effect on the effective mass splitting. The above feature is displayed also in Fig. 14(b), where the effective mass is plotted as a function of u. It is worth pointing out that, in case g_2, an almost linear relation between m_τ^*/m and I is hold even for high values of I (in comparison with the case g_1). So, the relation (33) with $c_2 = 0$ clearly describes the above dependence.

It should be emphasized that according to Figs. 12 and 13, the density dependence of the symmetry energy influences the values and also the slope of the effective mass (both for proton and neutron) but does not affect the sign of the mass splitting, which always remains positive (case g_1). Nevertheless, in case g_2, for different values of K the sign of the mass splitting may be negative or positive. In the case with $K = 180$ the positive slope of U_{sym} (see Fig. 7) is connected with the negative splitting [see Fig. 14(a)]. This result is in accordance with the findings of Refs. [32,37].

From the above analysis one can conclude that, in general, and by applying the proposed, in the present momentum effective interaction model, the slope (positive or negative) of the U_{sym} as a function of E_{kin} is not connected directly with the sign of the effective mass splitting. Certainly, there is a connection between the above quantities in the sense that both, according to Eqs. (27), (28), and (24), depend in a similar way on the parameters C_i, Z_i, Λ_i.

IV. SUMMARY

In this study we applied a momentum-dependent effective interaction to investigate the single-particle properties of hot asymmetric nuclear matter. More specifically, we have examined the single-particle potentials of protons and neutrons, the asymmetry potential, and the isospin mass splitting for various cases. The effects of the specific parametrization of the interaction part of the energy on the single-particle properties are studied and analyzed. It has been concluded that the behavior of the symmetry potential depends strongly on the parametrization of the interaction part of the energy density as well as on the momentum dependence of the regulator function. The effects of the parametrization are less pronounced on the isospin mass splitting. The effect of an increase of the temperature is just to shift higher the values of the proton and neutron single-particle potential. The symmetry potential U_{sym} can be an increasing or decreasing function of the nucleon kinetic energy, depending on the parametrization of the momentum-dependent effective interaction model. In the first case U_{sym} increases with the temperature, whereas in the second one the inverse behavior is observed.

[1] Madappa Prakash, I. Bombaci, Manju Prakash, P. J. Ellis, J. M. Lattimer, and R. Knorren, Phys. Rep. **280**, 1 (1997).

[2] W. A. Küpper, G. Wegmann, and E. R. Hilf, Ann. Phys. (NY) **88**, 454 (1974).

[3] D. Q. Lamb, J. M. Lattimer, C. J. Pethick, and D. G. Ravenhall, Nucl. Phys. **A360**, 459 (1981).

[4] H. Müller and B. D. Serot, Phys. Rev. C **52**, 2072 (1995).

[5] P. Danielewicz, R. Lacey, and W. G. Lynch, Science **298**, 1592 (2002).

[6] *Isospin Physics in Heavy-Ion Collisions at Intermediate Energies*, edited by Bao-An Li and W. Udo Schröder (Nova Science, New York, 2001).

[7] J. Xu, L. W. Chen, B. A. Li, and H. R. Ma, Phys. Lett. **B650**, 348 (2007).

[8] J. Xu, L. W. Chen, B. A. Li, and H. R. Ma, Phys. Rev. C **77**, 014302 (2008).

[9] J. Xu, L. W. Chen, B. A. Li, and H. R. Ma, Phys. Rev. C **75**, 014607 (2007).

[10] B. A. Li and L. W. Chen, Phys. Rev. C **74**, 034610 (2006).

[11] V. K. Mishra, G. Fai, L. P. Csernai, and E. Osnes, Phys. Rev. C **47**, 1519 (1993).

[12] L. P. Csernai, G. Fai, C. Gale, and E. Osnes, Phys. Rev. C **46**, 736 (1992).

[13] W. Zuo, Z. H. Li, A. Li, and G. C. Lu, Phys. Rev. C **69**, 064001 (2004).

[14] S. J. Lee and A. Z. Mekjian, Phys. Rev. C **63**, 044605 (2001); **77**, 054612 (2008).

[15] C. Das, R. Sahu, and A. Mishra, Phys. Rev. C **75**, 015807 (2007).

[16] W. Zuo, Z. H. Li, U. Lombardo, G. C. Lu, and H.-J. Schulze, Phys. Rev. C **73**, 035208 (2006).

[17] H. Huber, F. Weber, and M. K. Weigel, Phys. Rev. C **57**, 3484 (1998).

[18] C. Das, R. Sahu, and R. K. Tripathi, Phys. Rev. C **48**, 1056 (1993); C. Das, R. K. Tripathi, and R. Sahu, *ibid.* **45**, 2217 (1992); C. Das and R. Sahu, Phys. Lett. **B289**, 217 (1992).

[19] D. Bandyopadhyay, C. Samanta, S. K. Samadar, and J. N. De, Nucl. Phys. **A511**, 1 (1990).

[20] P. K. Jena and L. P. Singh, Phys. Rev. C **70**, 045803 (2004).

[21] Ch. C. Moustakidis, Phys. Rev. C **76**, 025805 (2007).

[22] C. Gale, G. Bertsch, and S. Das Gupta, Phys. Rev. C **35**, 1666 (1987).

[23] C. Gale, G. M. Welke, M. Prakash, S. J. Lee, and S. Das Gupta, Phys. Rev. C **41**, 1545 (1990).

[24] G. F. Bertsch and S. Das Gupta, Phys. Rep. **160**, 189 (1988).

[25] M. Prakash, T. T. S. Kuo, and S. Das Gupta, Phys. Rev. C **37**, 2253 (1988).

[26] I. Bombaci, EOS for isospin-asymmetric nuclear matter for astrophysical applications; in Ref. [6], pp. 35–81.

[27] C. B. Das, S. Das Gupta, C. Gale, and B. A. Li, Phys. Rev. C **67**, 34611 (2003).

[28] B. A. Li, C. B. Das, S. Das Gupta, and C. Gale, Nucl. Phys. **A735**, 563 (2004).

[29] L. W. Chen, C. M. Ko, and B. A. Li, Phys. Rev. Lett. **94**, 032701 (2005).

[30] P. E. Hodgson, *The Nucleon Optical Model* (World Scientific, Singapore, 1994).

[31] J. P. Jeukenne, A. Lejeune, and C. Mahaux, Phys. Rep. **25**, 83 (1976).

[32] V. Baran, M. Colonna, V. Greco, and M. Di Toro, Phys. Rep. **410**, 335 (2005).

[33] J. P. Jeukenne, A. Lejeune, and C. Mahaux, Nucl. Phys. **A245**, 411 (1975).

[34] R. B. Wiringa, Phys. Rev. C **38**, 2967 (1988).

[35] P. Danielewicz, Nucl. Phys. **A673**, 375 (2000).

[36] I. Bombaci and U. Lombardo, Phys. Rev. C **44**, 1892 (1991).

[37] B. A. Li, Phys. Rev. C **69**, 064602 (2004).

[38] W. Zuo, I. Bombaci, and U. Lombardo, Phys. Rev. C **60**, 024605 (1999).

[39] W. Zuo, L. G. Cao, B. A. Li, U. Lombardo, and C. W. Shen, Phys. Rev. C **72**, 014005 (2005).

[40] W. Zuo, U. Lombardo, H.-J. Schulze, and Z. H. Li, Phys. Rev. C **74**, 014317 (2006).

[41] F. Sammarruca, W. Barredo, and P. Krastev, Phys. Rev. C **71**, 064306 (2005).

[42] J. Rizzo, M. Colonna, M. Di Toro, and V. Greco, Nucl. Phys. **A732**, 202 (2004).

[43] J. Rizzo, M. Colonna, and M. Di Toro, Phys. Rev. C **72**, 064609 (2005).

[44] M. Di Toro, S. J. Yennello, and B. A. Li, Eur. Phys. J. A **30**, 153 (2006).

[45] E. N. E. van Dalen, C. Fuchs, and Amand Faessler, Phys. Rev. C **72**, 065803 (2005); Phys. Rev. Lett. **95**, 022302 (2005); Nucl. Phys. **A744**, 227 (2004).

[46] B. A. Li and L. W. Chen, Phys. Rev. C **72**, 064611 (2005).

[47] B. A. Li, C. B. Das, S. Das Gupta, and C. Gale, Phys. Rev. C **69**, 011603(R) (2004).

[48] B. Behera, T. R. Routrary, and R. K. Satpathy, J. Phys. G: Nucl. Part. Phys. **24**, 2073 (1998).

[49] B. Behera, T. R. Routrary, A. Praghan, S. K. Patra, and P. K. Sahu, Nucl. Phys. **A753**, 367 (2005); B. Behera, T. R. Routrary, B. Sahoo, and R. K. Satpathy, *ibid.* **A699**, 770 (2002).

[50] L. W. Chen, C. M. Ko, and B. A. Li, Phys. Rev. C **76**, 054316 (2007).

[51] L. W. Chen, C. M. Ko, and B. A. Li, Phys. Rev. C **72**, 064606 (2005).

[52] Z. H. Li, L. W. Chen, C. M. Ko, B. A. Li, and H. R. Ma, Phys. Rev. C **74**, 044613 (2006).

[53] M. Kutschera, Phys. Lett. **B340**, 1 (1994); Z. Phys. A **348**, 263 (1994); Acta Phys. Pol. B **29**, 25 (1998); S. Kubis and M. Kutschera, Nucl. Phys. **A720**, 189 (2003).

[54] B. A. Li, Phys. Rev. Lett. **88**, 192701 (2002).

[55] C. Fuchs and H. H. Wolter, Eur. Phys. J. A **30**, 5 (2006).

[56] N. K. Glendenning, *Compact Stars: Nuclear Physics, Particle Physics, and General Relativity* (Springer-Verlag, New York, 1997).

[57] D. V. Shetty, S. J. Yennello, and G. A. Souliotis, Phys. Rev. C **75**, 034602 (2007); **76**, 024606 (2007).

[58] M. B. Tsang *et al.*, Phys. Rev. Lett. **92**, 062701 (2004).

[59] C. H. Lee, T. T. S. Kuo, G. Q. Li, and G. E. Brown, Phys. Rev. C **57**, 3488 (1998).

[60] F. Sammarruca and P. Liu, arXiv:0806.1936 [nucl-th] (2008) (unpublished).

[61] A. M. Lane, Nucl. Phys. **35**, 676 (1962).

[62] R. Kozack and D. G. Madland, Phys. Rev. C **39**, 1461 (1989); Nucl. Phys. **A509**, 664 (1990).

[63] T. Lesinski, K. Bennaceur, T. Duguet, and J. Meyer, Phys. Rev. C **74**, 044315 (2006).

[64] B. A. Li, C. M. Ko, and Z. Z. Ren, Phys. Rev. Lett. **78**, 1644 (1997).

[65] B. A. Li, L. W. Chen, and C. M. Ko, Phys. Rep. **464**, 113 (2008).

[66] S. K. Bogner, R. J. Furnstahl, S. Ramanan, and A. Schwenk, Nucl. Phys. **A784**, 79 (2007).